PROCEEDINGS OF SPIE

MIRC-X polarinterferometry at CHARA

Setterholm, Benjamin, Monnier, John, Le Bouquin, Jean-Baptiste, Anugu, Narsireddy, Labdon, Aaron, et al.

MIRC-X polarinterferometry at CHARA

Benjamin R. Setterholm[a], John D. Monnier[a], Jean-Baptiste Le Bouquin[b], Narsireddy Anugu[c], Aaron Labdon[d], Jacob Ennis[a], Keith J. C. Johnson[e], Stefan Kraus[d], and Theo ten Brummelaar[f]

[a]Department of Astronomy, University of Michigan, Ann Arbor, MI 48109, USA
[b]Institut de Planétologie et d'Astrophysique de Grenoble, CNRS, Univ. Grenoble Alpes, FR
[c]Steward Observatory, University of Arizona, Tucson, AZ 85721, USA
[d]School of Physics and Astronomy, University of Exeter, Exeter, EX4 4QL, UK
[e]Department of Computer Sciences, University of Wisconsin, Madison, WI 53706, USA
[f]The CHARA Array, Mount Wilson Observatory, Mount Wilson, CA 91023, USA

ABSTRACT

We present a new polarimetric mode for the MIRC-X 6-telescope beam combiner at CHARA. Utilizing the extensive $u - v$ coverage afforded by CHARA this mode will be able to resolve and constrain scattered light in environs at milliarcsecond separations of target stars, a largely unexplored parameter space to-date in astronomy. Notably, this upgrade will allow for the investigation of the scattering properties of the inner dust wall at the sublimation radius of Herbig Ae/Be star disks, dust shells surrounding evolved stars, and gas-rich disks around Be stars. Our design adds a series of rotating half-wave plates, achromatic across J- and H-bands, and a polarizing beamsplitter into the MIRC-X beam path. In this work, we also preview on-sky observations, discussing ongoing work calibrating instrumental polarization effects in the CHARA beam path as well as upgrades to the MIRC-X data reduction pipeline.

Keywords: interferometry, polarimetry, infrared, protoplanetary disks, stellar disks, scattered light

1. INTRODUCTION

Whereas polarization measurements are commonplace in radio interferometry,[1] they are considerably more difficult to conduct at visible and near-infrared (NIR) wavelengths. The first attempts at optical polarinterferometric observations occurred at Narrabri Observatory, investigating coronal polarization in the hot supergiant star β Ori. However, the predicted signal was over an order of magnitude smaller than the measurement uncertainty, and no polarization dependent variation was observed.[2] This experiment was later repeated again for α Lyr at the CERGA interferometer[3] and γ Cas at GI2T,[4] though these too failed to detect polarimetric variation owing to poor signal-to-noise ratio (SNR). The first successful optical polarinterferometric observations were conducted with the Sydney University Stellar Interferometer, detecting the scattering signature of dust surrounding the Mira variable stars R Car and RR Sco.[5] Aperture masking polarinterferometry has also been successfully used at VLT to study AGB stars, finding a scattering signature of large transparent dust grains (300 nm average radius) located around 2 stellar radii away from three target sources;[6] this technique is further employed for studies of protoplanetary disks with the VAMPIRES instrument at the Subaru telescope.[7,8]

This paper describes a new hardware subsystem and accompanying software ecosystem update for MIRC-X,[9] a near-infrared interferometric beam combiner installed at the CHARA array. Combining light from all six 1-meter telescopes in the array simultaneously, MIRC-X is capable of observing targets as faint as $m_H \approx 7.5$ with milliarcsecond or better typical spatial resolution. The new mode, described herein, allows for polarimetric observations to be conducted in H-band (1.50–1.73 μm) at low spectral resolution, typically $\lambda/\Delta\lambda \approx 50$. This mode augments the existing MIRC-X beam train with additional optics at two locations: a Wollaston prism (polarizing beamsplitter) inserted just prior to the instrument camera – formerly used only for internal calibration and not offered for science proposals – and a set of controllable retarders placed at the head of the instrument. The retarders, approximately achromatic half-wave plates across J- and H-bands, are used to control the sky-frame polarization basis to which the Wollaston prism is sensitive to, allowing the direction and degree of polarization of the target of interest along each baseline to be measured.

Further author information: (Send correspondence to B.R.S.)
B.R.S.: E-mail: bensett@umich.edu

The second section of this paper explores a sample of science cases that stand to uniquely benefit from high angular-resolution polarimetric observations. The third section details the hardware design and optical implementation into the MIRC-X beam path. The fourth section outlines the software design and integration with the existing observing and data reduction tools. In the following section, the instrumental testing and calibration is explained and the data quality of a sample observation is assessed. Finally, we summarize the progress of the project and layout the remaining steps we plan to complete to make this mode ready for community use.

2. SCIENCE MOTIVATION

2.1 Planet-forming disks

Young stellar object (YSO) disks are nurseries for forming exoplanetary systems. Scattered-light coronographic imaging surveys, utilizing polarimetric instruments on today's 10-meter class observatories, have seen much success tracing dust distributions and features on ∼10 au scales in these disks, critical to modeling the dynamics leading to gas giant planets. However, in order to examine sub-au scale structures of these disk systems, necessary for accurately modeling terrestrial planet formation, the use of long-baseline interferometry is required. The new MIRC-X polarization mode will be able to extend scattered light observations conducted routinely with solitary telescopes into the terrestrial planet regime of a handful of nearby YSO disks.

Of particular interest is whether a substantial population of dust lies within the putative sublimation radius of typical astrosilicate grains, where the disk equilibrium temperature exceeds 1800 K. Interferometric observations indicate that a significant fraction (up to a third) of the total near-infrared (NIR) excess disk flux in some YSO systems originates within this radius.[10–15] If this emission is polarized, it would indicate the presence of refractory grains scattering incident starlight into the line of sight, whereas the absence of polarized emission would be evidence that this region is dominated by an optically-thick gas. Either conclusion will have significant impact on models of terrestrial planet formation and stellar accretion of pre-main-sequence stars.

Figure 1 simulates what a MIRC-X polarimetric observation might look like for Herbig Ae star HD 163296, assuming toy-model a Gaussian disk geometry[14] with 20 % radial polarized emission.

2.2 Evolved stars

High mass stars undergo significant mass loss, especially during post-main-sequence stages in their evolution. Winds driven from the stellar atmospheres condense to form astrosilicate dust grains, enveloping their host stars. The details of the physical mechanisms driving this mass loss is not yet well understood. High spatial resolution measurements are required to probe the crucial physics occurring within a few stellar radii of the host star.[16] Mira variables are an especially compelling class of evolved star, as they undergo periodic pulsations ejecting large amounts of material which quickly precipitates into dust grains[17] and many should produce a significant polarization signal; indeed the first successful polarinterferometry measurements detected a signal in differential visibilities around two Mira variable stars.[5] Resolved red supergiant stars, such as Betelgeuse which recently underwent a period of unprecedented dimming likely due to ejection of large grains,[18] as well as AGB stars, which have been observed to contain polarized emission from dust shells within a few stellar radii of their photospheres,[6] will also make for compelling targets. The MIRC-X polarimetric mode will make it possible to spatially probe dusty structures in the shells surrounding evolved stars, allowing detailed characterization of their geometry and evolution.

2.3 Be stars

Be stars are non-supergiant (primarily, but not exclusively, main-sequence) early-type stars, typically with spectral type B, which have at some point been observed with prominent Balmer line emission (not necessarily continuously). These stars typically exhibit strong infrared excess, strong linearly polarized emission, and short-term time-variability owing to a hot gaseous circumstellar disk with strong Thompson scattering.[19,20] While the scattering is more prominent at shorter wavelengths, there may be sufficient scattering contribution in the near-infrared of some Be star objects for a measurable polarimetric signal to be detected by the MIRC-X polarimetric mode. Such a signal could then be used to further constrain the chemical and geometrical structure of the circumstellar disks.
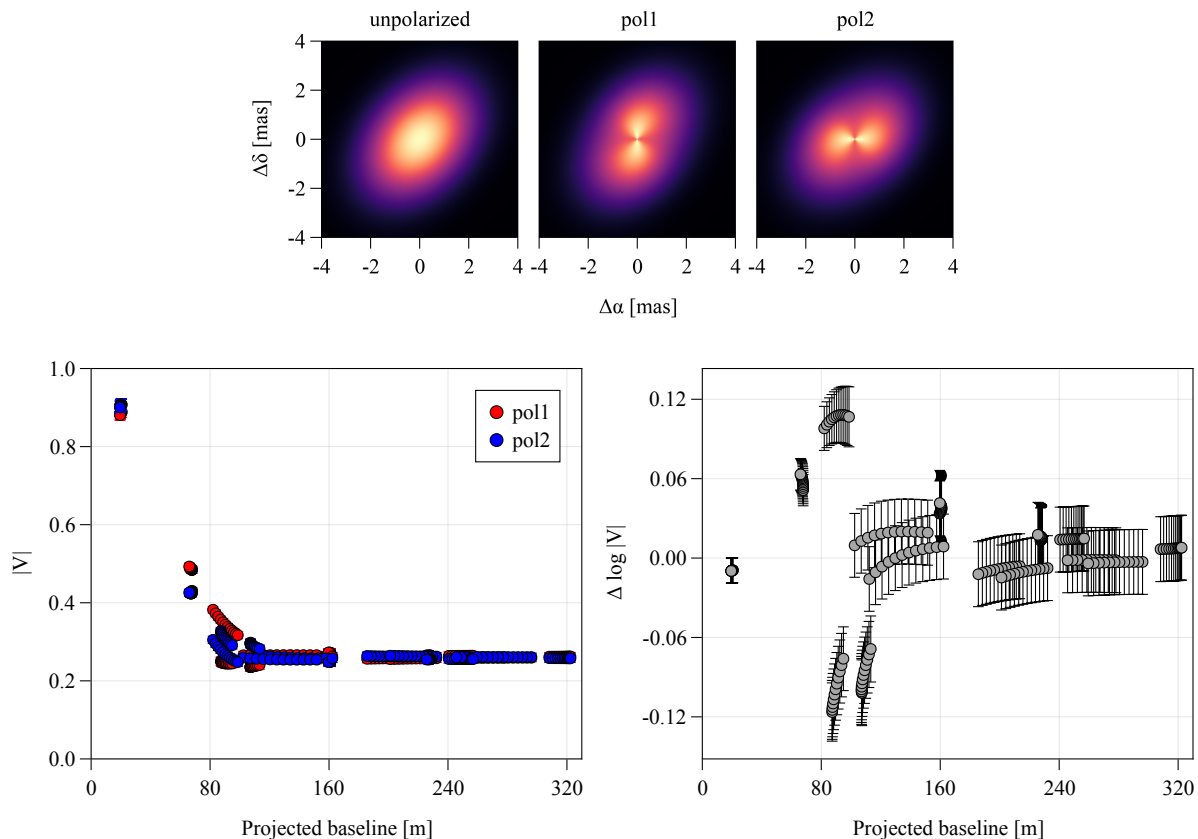
Figure 1. A simulated MIRC-X polarimetric observation of YSO star HD 163296 at 1.6 μm, assuming a toy model Gaussian circumstellar disk with 20 % radial linear polarization. Top: "Images" of the modeled disk[14] in unpolarized and polarized emission. Bottom left: Modeled polarized visibility amplitudes for 6 telescope observations based on typical CHARA $u - v$ coverage for this star. Bottom right: Differential polarized visibility amplitude (pol1/pol2 plotted in log scale) for the same synthetic measurements, with conservative error estimates (higher SNR is expected after proper calibration). Our simulations of various disk models indicate that a clear signal should be observable at intermediate baselines.

3. HARDWARE

The MIRC-X polarimetric mode augments the existing instrument with several new mechanical and optical elements, described in detail below. Photographs of the hardware installed in the instrument beam path are provided in Figure 2. Figure 3 diagrams the beam-path and layout of major components on the MIRC-X optical bench and highlights the placement of the polarimetric mode optics.

Placed in the optical path just prior to the camera is a custom quartz Wollaston prism, manufactured by United Crystals Inc. This beamsplitter separates ordinary and extraordinary rays at an angle of 1° at 550 nm, and was previously only used for internal instrument calibration of the MIRC-X lithium niobate plates. The ingress and egress surfaces of the optic are prepared with a broadband anti-reflection coating optimized for 1.0–1.8 μm wavelength light. The internal, cemented faces of two orthogonal prisms comprising the Wollaston are polished but not coated.

To facilitate measurements of the full linear polarization state, the new mode provides a user orientable, achromatic half-wave plate (HWP) for each CHARA beam. These 1-inch, air-spaced waveplates were custom manufactured by Wuhan Union Optic, Inc., designed to be performant throughout J and H bands (1.05–1.80 μm), with a retardance of 0.50 ± 0.01. Figure 4 shows the theoretical retardance performance as reported by the manufacturer. An antireflective coating was applied to both external faces of each half-wave plate, with total reflectance better than 1.5%. The throughput of each optic is better than 96% across the operating wavelength range. The total wavefront distortion is $\lambda/8$ at 633 nm (peak to valley).
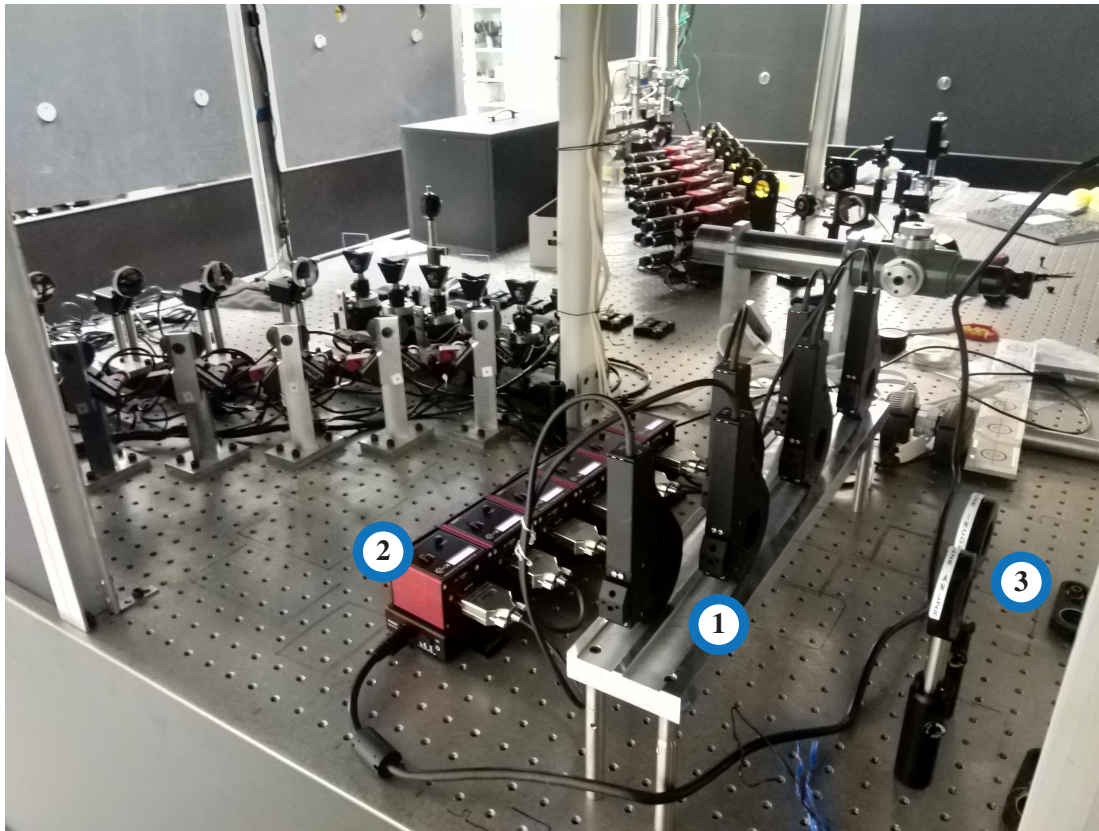
Figure 2. The new polarimetric hardware installed on the MIRC-X optical bench at CHARA. The top panel shows the half-wave plate assembly ① and motor control boxes ② in relation to the MIRC-X instrument during initial testing in 2019 November, where calibration was conducted with a pair of linear polarizers ③. Not pictured is the mini-PC, which is installed above the MIRC-X table, controlling the motor boxes via USB. The bottom panel shows the waveplates "beam-on" during on-sky observations in 2020 November.
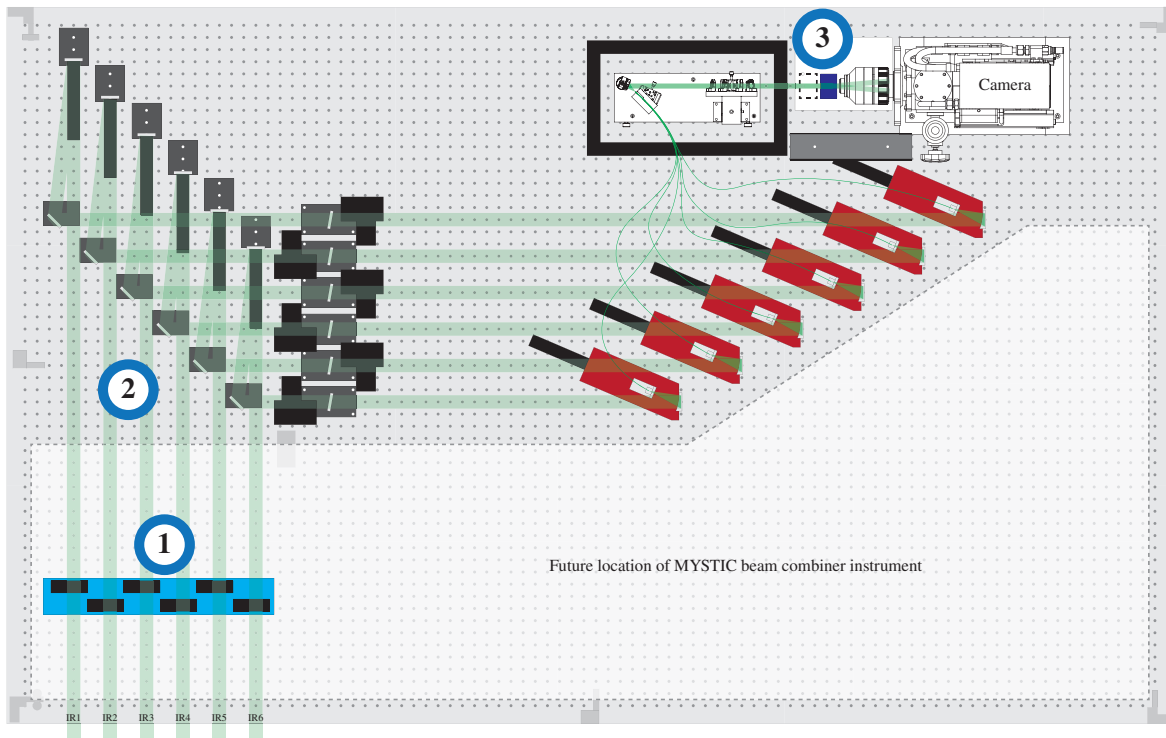
Figure 3. Layout of the major components in the MIRC-X instrument, with areas relevant to the polarimetric mode colored blue and labeled with numbered circles. Infrared beams entering the instrument from CHARA are shown in light green. The new half-wave plate assembly ①, highlighted in cyan, is the first MIRC-X element encountered by incoming beams. Pictured is the current installed location, though a new motorized mount will be designed and placed at ② when MYSTIC is installed (c. 2021 June). The Wollaston prism ③, highlighted in navy blue, is inserted immediately before the MIRC-X camera. The polarimetric dispersion angle of the light exiting the Wollaston prism is exaggerated in the figure for emphasis.
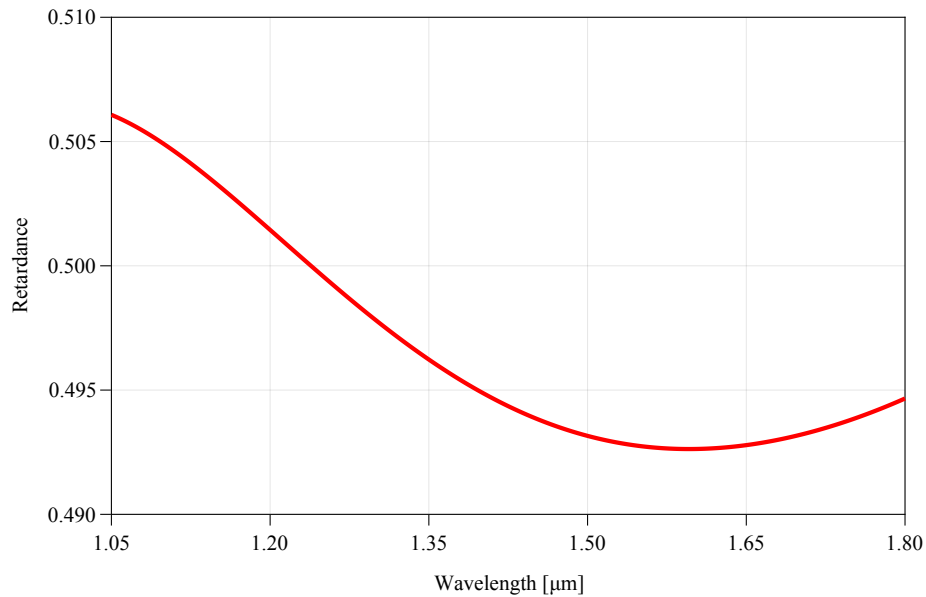

Figure 4. Theoretical retardance curve of the custom half-wave plates produced by Wuhan Union Optic, Inc., reproduced here with permission. The optics were verified by the manufacturer to meet the retardance specification of 0.50 ± 0.01 inside the wavelength range.

Each half-wave plate optic is installed in a ThorLabs Motorized Rotation Stage (ThorLabs PRM1Z8). All stages are mounted to a common interface plate that can be easily inserted and removed by hand on the optical bench. This whole assembly is placed prior to the MIRC-X lithium niobate plates, which compensate for relative phase shifts between beams induced by the instrument's polarization-maintaining single-mode fiber optics. In close proximity to the mount, below the CHARA beams, is a series of ThorLabs K-Cube (KDC101) motor controllers–one for each waveplate motor–mounted together on a powered USB hub (ThorLabs KCH601). This hub is connected via USB to a fanless mini-PC (ACEPC T11) placed on a shelf above the instrument which runs custom software for controlling the half-wave plate orientations (see §4.1).

In a perfect optical system, the output beams from a Wollaston prism after passing through a half-wave plate with a fast axis oriented vertically samples the vertical and horizontal polarization states, and with fast axis oriented at 22.5° samples the diagonal and anti-diagonal polarization states. Further rotating the half-wave plate to 45° and 67.5° positions samples the same polarization bases again respectively, but with the measured states of the two Wollaston output beams swapped with respect to their 0° and 22.5° configuration. Since the CHARA system and waveplates themselves are not perfect, we recommend on-sky programs conduct measurements at all four listed positions in order to best estimate the linear polarization parameters.

To accommodate MYSTIC,[21] a K-band beam combiner which is scheduled to be commissioned on the MIRC-X optical bench in summer 2021, the half-wave plate mount assembly will be redesigned. Along with a revised footprint, the new interface plate will be mounted on a vertical, motorized elevator allowing observers to insert or remove the waveplates from the beam train with the click of a button.

4. SOFTWARE

4.1 Half-waveplate operations

The half-waveplate motor rotations are controlled by a custom C# program utilizing ThorLabs Kinesis DLLs on a mini-PC running Microsoft Windows 10 Professional. This software is installed as a Windows service, so it starts itself when the operating system boots (for example, after a power outage) and automatically restarts itself if its process is terminated. The program listens for short messages sent over the local network with the Transmission Control Protocol (TCP), interacts with the hardware, and then returns a status message over TCP. Implemented messages include commands to home a motor (`HOME`), move a motor to an absolute positions (`MOVE_ABS`), move a motor by a relative offset (`MOVE_REL`), halt a motor's motion (`ABORT`), and to query a motor's angular position and whether the motor is moving or stationary (`STATUS`). Command messages each apply to a single motor, numbered 1–6 corresponding to the MIRC-X beam it is in, which is included as a part of the message. If the message is a move command, the desired offset in degrees is included as well. Message components are separated by pipe characters and each message ends with a null terminator. Incoming command messages are parsed, command execution is initiated, and then the program immediately returns a status message (or an error message if the incoming command is not recognized or invalid). Command messages are processed one at a time, but can be received in rapid succession; multiple motors can be moving simultaneously.

A new server, `mircx_hwp_server`, is implemented in the MIRC-X software ecosystem[9] to mediate all communication between the internal CHARA messages protocol and the motor controlling mini-PC. Since it was not possible to manually install the bare optic HWPs into the motors such that their fast axes are perfectly vertical with the motors at their home positions, the `mircx_hwp_server` converts a user input angle relative to vertical into a home referenced angle for each motor, performing any 360° wrappings as needed. From an observers perspective, a few additional widgets are added to the MIRC-X super server GUI window, allowing the user to select an initial waveplate position, a rotation offset "step" angle, and a number of steps in an observation sequence (see Figure 5). The `mircx_super_server` then sequences the data and shutter observations and requests the `mircx_hwp_server` to move the HWPs together to the desired positions. Background files are only collected at the initial waveplate position, and the beam sequence exposes each CHARA beam individually for a single waveplate position before moving on to the next position. The saved FITS headers contain the recorded waveplate position angle and motor home position for each beam with respect to a vertical waveplate orientation ("`HIERARCH MIRC HWPn POS`" and "`HIERARCH MIRC HWPn REF`" respectively, where n is the motor number minus 1*).

---

*The FITS header entries follow a 0-indexed numbering convention in concurrence with header entries for other motors in the MIRC-X system. However, colloquially, these motors are referred to according to the CHARA beam they are inserted into, which follows a 1-indexed numbering scheme.
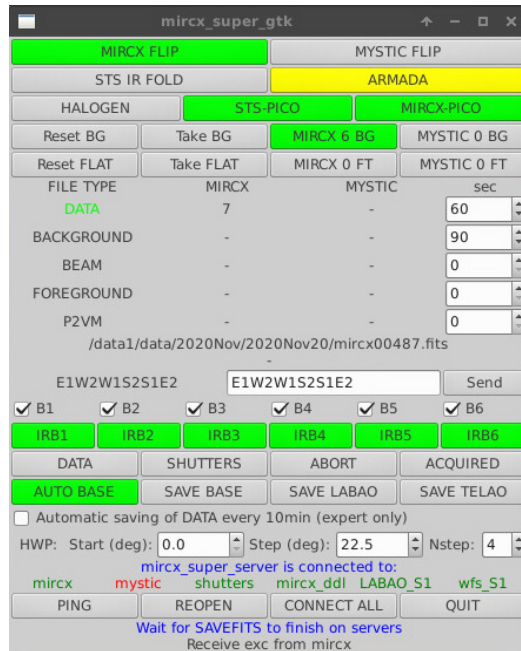
Figure 5. The "Super" GUI is the main data sequencer for the MIRC-X and upcoming MYSTIC instruments. For the polarimetric mode, a new line of widgets has been added near the bottom of the window, allowing a user to select initial half-wave plate positions as well as to automate data collection for multiple positions in a sequence. All 6 motor axes are controlled in tandem.

The `mircx_gdt_server` GUI allows the observer to choose which of the two recorded polarization states is used for group delay optimization. Tracking may also be conducted on the sum of the states in each wavelength channel, simulating standard non-polarimetric MIRC-X observations. Figure 6 demonstrates fringe tracking for a typical on-sky observation.

4.2 Polarimetric data reduction

We are in the process of upgrading the MIRC-X data reduction pipeline[†] to fully process polarized data. In the current version of the pipeline (v-1.3.x), an early step identifies the locations of the photometric channels and the interference fringes in the raw FITS file. Much of the software has been designed under the assumption that there can be only a single window for each of these. Since the Wollaston prism creates two sets of photometry and fringes on the detector, the pipeline terminates prematurely with an error.

To circumvent this issue in the short-term, a preprocessing script `mircx_polsplit.py` is available with the pipeline code which, when applied to a directory of polarization data, splits the data in each FITS file into two files based on the detector read-out mode windowing, one for each polarization state. The split files are saved in new directories `pol1/` and `pol2/` inside the parent directory; the original files are not removed in the process. The parent file's FITS header is duplicated verbatim for each of the split files. The current version of the data reduction pipeline can then be run individually on each of the resulting directories to extract square visibility and closure triangle information.

We are in the process of revising the architecture of the pipeline to extract polarization differential quantities, such as differential visibility phase, in addition to standard interferometric measurements. These routines will identify and compare fringes of both states simultaneously, correcting for slightly non-equal spectral dispersion seen in the for the two polarization measurements. We will make use of the HWP positions of subsequent files and the sky parallactic angle of each measurement to estimate linear Stokes parameters for each differential visibility measurement in the final data product.

[†]The data pipeline is available in a public git repository at https://gitlab.chara.gsu.edu/lebouquj/mircx_pipeline.
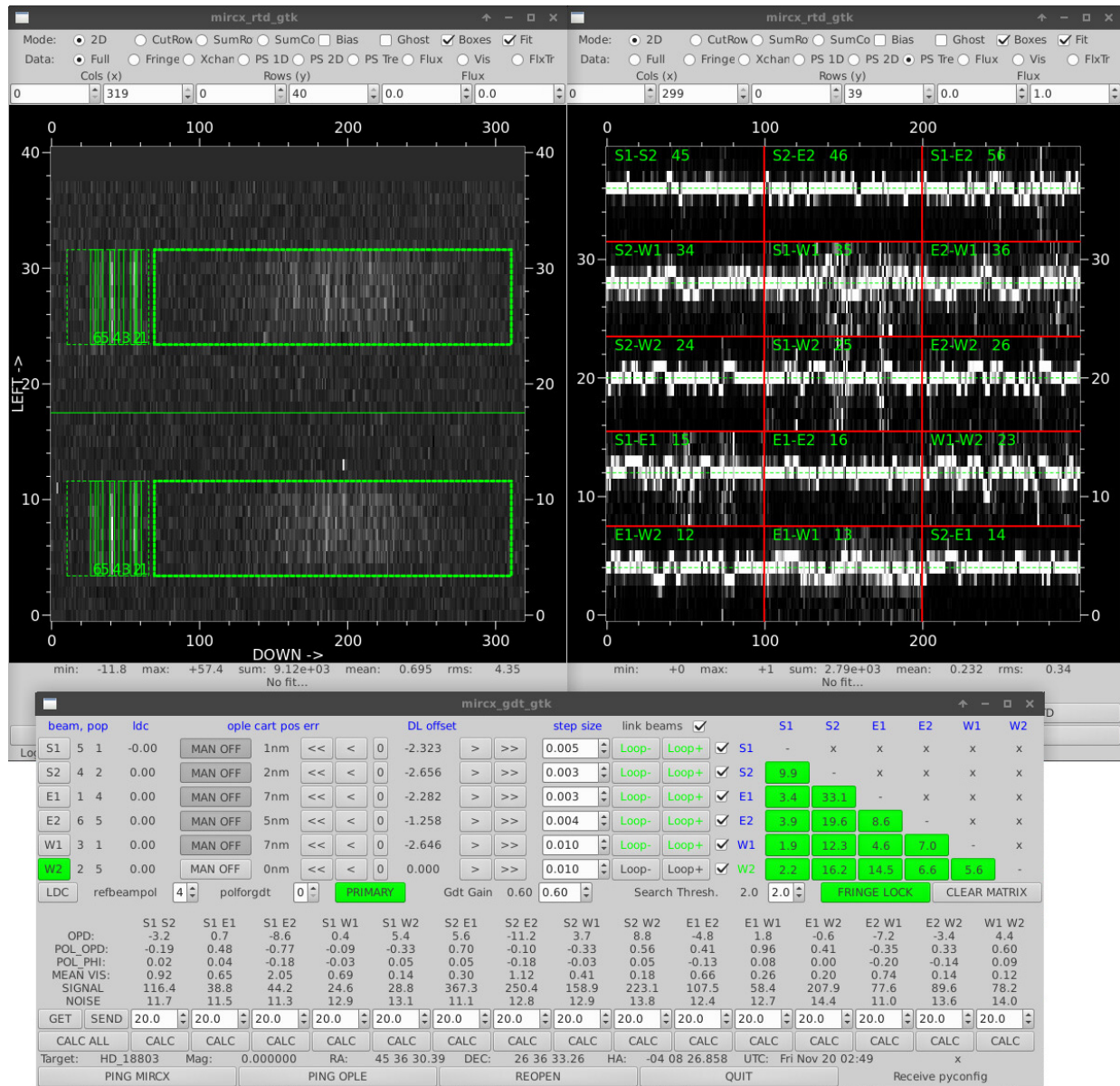
Figure 6. Example six telescope observation of a target with all 15 baseline fringes locked and tracked. Top left: Snapshot of the detector readout. Bottom: Group delay tracker GUI. Note the `polforgdt` spin-box; "1" and "2" are used to track group delay for the top or bottom polarization states, and "0" is used to track the sum. Top right: Locked and tracked fringes over time.

5. OBSERVING TARGETS ON-SKY

5.1 Calibration

Practical application of the technique of long-baseline interferometry usually necessitates many reflections at large scattering angles in order to direct all beams together from array telescopes, through optical path length correction, to final beam combination. CHARA is no exception, with each beam undergoing 19 reflections and 1 refraction before it even reaches the MIRC-X instrument optics, whereupon it undergoes additional reflections and refractions. Each interaction with an optical element along the beam changes the polarization state of the light, up to the few percent level, with large angle-of-incidence reflections having a greater effect on the overall change in polarization. Therefore, detailed characterization of the instrumental polarization is crucial in order to correct observations and extract polarimetric measurements for on-sky sources.

The beam paths in the CHARA array itself were designed with homologous reflections in each arm[22] so that the resulting polarization state remains consistent across all beams.[23,24] Nevertheless, diattenuation effects and phase shifts accumulated from all reflections in CHARA and MIRC-X induces an instrumental polarization in the measured fringes at the detector that must be accounted for in order to measure the polarization of the on sky source adequately. Schematically, the initial polarization state P_i of every photon before it reaches the array, given by a Jones vector defined by coordinates in the right ascension and declination directions on-sky, is modified by the optical elements in the beam paths, represented by a multiplied series of 2×2 matrices, and has polarization state P_f at the detector. Equation 1 outlines this transformation, where $\mathbf{M}_{MX}$ is the matrix describing the polarization of the MIRC-X instrument, $\mathbf{WP}(\zeta, \theta)$ describes the contribution of the half-wave plates as a function of their orientation angle θ and retardance $2\pi\zeta$ (expanded in Equation 2), and the $\mathbf{R}$s are appropriate rotation matricies for the azimuth A, altitude a, and parallactic angle q. The remainder of the normalized matrices include complex elements subscripted by their CHARA mirror numbers and account for the net diattenuation and relative phase delay introduced by these mirrors. Finally, the f and ϕ terms encapsulate the net flux and bulk phase shift of the entire beam-path, respectively. We note also that these matrix terms have slight wavelength dependence.

$$\begin{pmatrix} P_{f,1} \\ P_{f,2} \end{pmatrix} = f \cdot e^{i\phi} \mathbf{M}_{MX} \mathbf{WP}(\zeta, \theta) \begin{pmatrix} 1 & 0 \\ 0 & \widetilde{M}_{8-19} \end{pmatrix} \mathbf{R}(A) \begin{pmatrix} 1 & 0 \\ 0 & \widetilde{M}_{4-7} \end{pmatrix} \mathbf{R}(a) \begin{pmatrix} 1 & 0 \\ 0 & \widetilde{M}_{1-3} \end{pmatrix} \mathbf{R}(q) \begin{pmatrix} P_{i,\alpha} \\ P_{i,\delta} \end{pmatrix} \quad (1)$$

$$\mathbf{WP}(\zeta, \theta) = \mathbf{R}(\theta) \begin{pmatrix} 1 & 0 \\ 0 & e^{i\zeta} \end{pmatrix} \mathbf{R}(-\theta) \quad (2)$$

The coefficients of the $\mathbf{M}_{MX}\mathbf{WP}(\zeta, \theta)$ terms for each beam are measured directly by placing a linear polarizer immediately upstream of the half-wave plate and using the CHARA internal light source (the Six Telescope Simulator[9]) to measure the resultant flux ratio between polarization states at the detector for various positions of the half-wave plate and linear polarizer. This set-up be seen in the lower right of the top panel of Figure 2.

We are now working to estimate the remainder of the coefficients using on-sky measurements of a number of (nearly all unpolarized) sources across the sky. Each CHARA beam may have one of 5 positions for its Pipes of Pan (PoP) mirror, M_{11}, used in optical delay compensation for the array. We assume the changes in the PoP configuration have a negligible effect on the final polarization state as all these mirrors are nearly normal to the incident rays and coated in the same manner. Once the matrix coefficients are all estimated, they will be incorporated into the data reduction pipeline.

5.2 On-sky demonstration

Inaugural on-sky observations with the Wollaston prism were conducted over 2 nights in 2019 June. After the waveplates were delivered to CHARA, full MIRC-X polarimetric mode observations were conducted over the course of 5 nights from 2019 November to 2020 November, targeting a few different YSO objects. Fringes were exposed on the detector for a sequence 1 minute at each of four half-wave plate orientations – 0°, 22.5°, 45°, and 67.5° – repeating the pattern a number of times. For each science target, 1–3 (presumably unpolarized) calibrator stars were observed at close declinations and hour angles to the science target for instrumental polarization calibration and for estimating the transfer function for the particular region of the atmosphere. A sample observation is shown in Figure 7.

In addition to science data, we have observed a few known unpolarized calibrator stars at different locations on the sky in order to aid in extracting the matrix coefficients describing the CHARA internal instrumental polarization. We have requested followup observations of science and science calibrator targets at traditional, single-telescope polarimeter facilities to further this modeling.

6. SUMMARY AND FUTURE WORK

We have developed a new 6-telescope (15 baseline) polarimetric mode for the CHARA interferometer, augmenting the existing MIRC-X instrument with additional hardware. This mode makes available milliarcsecond-scale H-band polarimetric measurements of a variety of stellar phenomena, a largely unexplored window on the universe. Control of this new hardware has been tested with the CHARA/MIRC-X software ecosystem, and current work is in progress to characterize and calibrate the intrinsic instrumental polarization of CHARA and MIRC-X as well as to upgrade the data pipeline to smoothly process observations made with this this mode. We hope to have these tasks completed by summer 2021, in tandem with the installation of the forthcoming MYSTIC instrument. During this time, we will move the waveplates introduced with
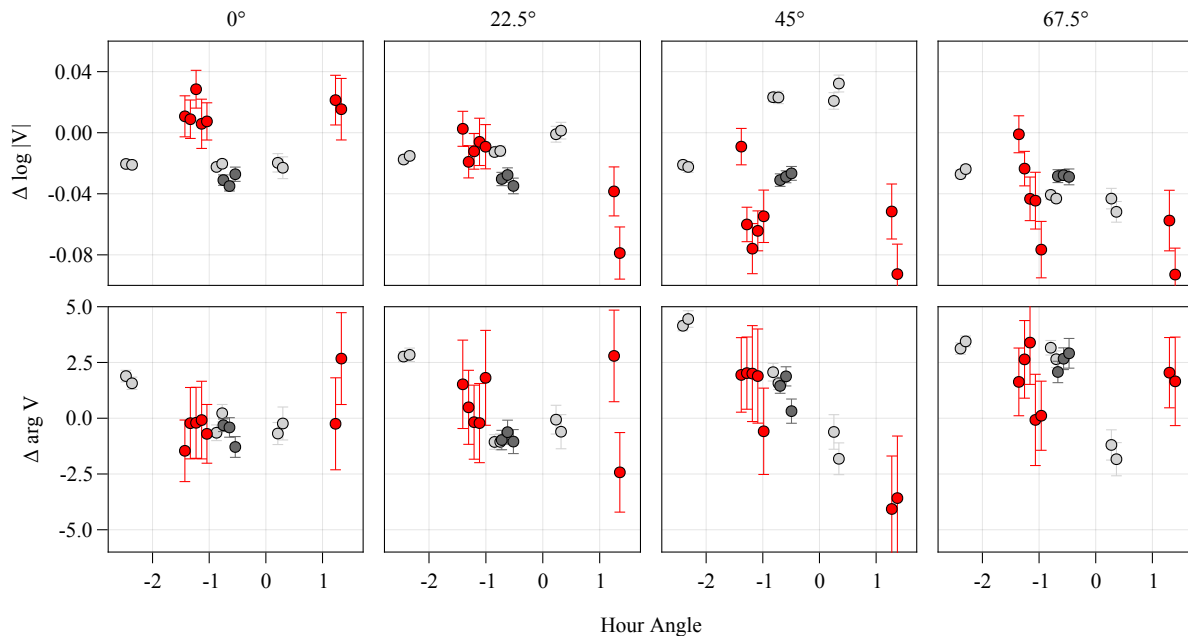
Figure 7. Sample MIRC-X polarimetric measurements of a YSO (red) and two calibrator stars (light/dark gray) on 2019 November 10 for the E2-W2 (approx. 150 m) baseline at 1.6 μm, plotted by time of observation. Top: differential visibility amplitude of pol1/pol2 for each HWP angle position measured (plotted in log space). Bottom: differential visibility phases phases of pol1 − pol2. While there does appear to be a signal in the data, the temporal variations in the calibrator stars still need to be corrected by calibrating CHARA's internal polarization before we can extract a final polarization measurement for the YSO (see §5.1). Unpolarized calibrator stars should have an intrinsic differential visibility amplitude of unity and differential visibility phase of zero (after correcting for instrumental effects).

the polarization mode onto a (yet to be designed) motorized mount, allowing observers to queue polarimetric observations on-demand, without needing advanced daytime set-up in the CHARA beam combination lab. Beyond summer 2021, we plan to eventually make available J-band observations with this mode. (Current progress on J-band commissioning[25] for MIRC-X, as well as a review of the current operations of the instrument,[26] are discussed elsewhere in these these proceedings).

REFERENCES

[1] Hamaker, J. P., Bregman, J. D., and Sault, R. J., "Understanding radio polarimetry. I. Mathematical foundations.," *A&AS* **117**, 137–147 (May 1996).

[2] Hanbury Brown, R., Davis, J., and Allen, L. R., "An attempt to detect a corona around beta Orionis with an intensity interferometer using linearly polarized light.," *MNRAS* **168**, 93–100 (July 1974).

[3] Vakili, F., "Study of stellar polarization with the CERGA interferometer," *A&A* **101**, 352–355 (Sept. 1981).

[4] Rousselet-Perraut, K., Vakili, F., Mourard, D., Morand , F., Bonneau, D., and Stee, P., "An attempt to detect polarization effects in the envelope of gamma Cassiopeiae with the GI2T interferometer," *A&AS* **123**, 173–177 (May 1997).

[5] Ireland, M. J., Tuthill, P. G., Davis, J., and Tango, W., "Dust scattering in the Miras R Car and RR Sco resolved by optical interferometric polarimetry," *MNRAS* **361**, 337–344 (July 2005).

[6] Norris, B. R. M., Tuthill, P. G., Ireland , M. J., Lacour, S., Zijlstra, A. A., Lykou, F., Evans, T. M., Stewart, P., and Bedding, T. R., "A close halo of large transparent grains around extreme red giant stars," *Nature* **484**, 220–222 (Apr. 2012).

[7] Norris, B., Schworer, G., Tuthill, P., Jovanovic, N., Guyon, O., Stewart, P., and Martinache, F., "The VAMPIRES instrument: imaging the innermost regions of protoplanetary discs with polarimetric interferometry," *MNRAS* **447**, 2894–2906 (Mar. 2015).

[8] Norris, B. R. M., Tuthill, P., Jovanovic, N., Lozi, J., Guyon, O., Cvetojevic, N., and Martinache, F., "Diffraction-limited polarimetric imaging of protoplanetary disks and mass-loss shells with VAMPIRES," in [*Advances in Optical Astronomical Instrumentation 2019*], *Society of Photo-Optical Instrumentation Engineers (SPIE) Conference Series* **11203**, 112030S (Jan. 2020).

[9] Anugu, N., Le Bouquin, J.-B., Monnier, J. D., Kraus, S., Setterholm, B. R., Labdon, A., Davies, C. L., Lanthermann, C., Gardner, T., Ennis, J., Johnson, K. J. C., Ten Brummelaar, T., Schaefer, G., and Sturmann, J., "MIRC-X: A Highly Sensitive Six-telescope Interferometric Imager at the CHARA Array," *AJ* **160**, 158 (Oct. 2020).

[10] Kraus, S., Preibisch, T., and Ohnaka, K., "Detection of an Inner Gaseous Component in a Herbig Be Star Accretion Disk: Near- and Mid-Infrared Spectrointerferometry and Radiative Transfer modeling of MWC 147," *ApJ* **676**, 490–508 (Mar. 2008).

[11] Tannirkulam, A., Monnier, J. D., Harries, T. J., Millan-Gabet, R., Zhu, Z., Pedretti, E., Ireland, M., Tuthill, P., ten Brummelaar, T., McAlister, H., Farrington, C., Goldfinger, P. J., Sturmann, J., Sturmann, L., and Turner, N., "A Tale of Two Herbig Ae Stars, MWC 275 and AB Aurigae: Comprehensive Models for Spectral Energy Distribution and Interferometry," *ApJ* **689**, 513–531 (Dec. 2008).

[12] Benisty, M., Natta, A., Isella, A., Berger, J.-P., Massi, F., Le Bouquin, J.-B., Mérand, A., Duvert, G., Kraus, S., Malbet, F., Olofsson, J., Robbe-Dubois, S., Testi, L., Vannier, M., and Weigelt, G., "Strong near-infrared emission in the sub-AU disk of the Herbig Ae star HD 163296: evidence of refractory dust?," *A&A* **511**, A74 (Feb. 2010).

[13] Lazareff, B., Berger, J. P., Kluska, J., Le Bouquin, J. B., Benisty, M., Malbet, F., Koen, C., Pinte, C., Thi, W. F., Absil, O., Baron, F., Delboulbé, A., Duvert, G., Isella, A., Jocou, L., Juhasz, A., Kraus, S., Lachaume, R., Ménard, F., Millan-Gabet, R., Monnier, J. D., Moulin, T., Perraut, K., Rochat, S., Soulez, F., Tallon, M., Thiébaut, E., Traub, W., and Zins, G., "Structure of Herbig AeBe disks at the milliarcsecond scale . A statistical survey in the H band using PIONIER-VLTI," *A&A* **599**, A85 (Mar. 2017).

[14] Setterholm, B. R., Monnier, J. D., Davies, C. L., Kreplin, A., Kraus, S., Baron, F., Aarnio, A., Berger, J.-P., Calvet, N., Curé, M., Kanaan, S., Kloppenborg, B., Le Bouquin, J.-B., Millan-Gabet, R., Rubinstein, A. E., Sitko, M. L., Sturmann, J., ten Brummelaar, T. A., and Touhami, Y., "Probing the Inner Disk Emission of the Herbig Ae Stars HD 163296 and HD 190073," *ApJ* **869**, 164 (Dec. 2018).

[15] Kluska, J., Berger, J. P., Malbet, F., Lazareff, B., Benisty, M., Le Bouquin, J. B., Absil, O., Baron, F., Delboulbé, A., Duvert, G., Isella, A., Jocou, L., Juhasz, A., Kraus, S., Lachaume, R., Ménard, F., Millan-Gabet, R., Monnier, J. D., Moulin, T., Perraut, K., Rochat, S., Pinte, C., Soulez, F., Tallon, M., Thi, W. F., Thiébaut, E., Traub, W., and Zins, G., "A family portrait of disk inner rims around Herbig Ae/Be stars. Hunting for warps, rings, self shadowing, and misalignments in the inner astronomical units," *A&A* **636**, A116 (Apr. 2020).

[16] Haubois, X., Norris, B., Tuthill, P. G., Pinte, C., Kervella, P., Girard, J. H., Kostogryz, N. M., Berdyugina, S. V., Perrin, G., Lacour, S., Chiavassa, A., and Ridgway, S. T., "The inner dust shell of Betelgeuse detected by polarimetric aperture-masking interferometry," *A&A* **628**, A101 (Aug. 2019).

[17] Gail, H.-P., Scholz, M., and Pucci, A., "Silicate condensation in Mira variables," *A&A* **591**, A17 (June 2016).

[18] Cotton, D. V., Bailey, J., Horta, A. D., Norris, B. R. M., and Lomax, J. R., "Multi-band Aperture Polarimetry of Betelgeuse during the 2019-20 Dimming," *Research Notes of the American Astronomical Society* **4**, 39 (Mar. 2020).

[19] Chesneau, O., Wolf, S., and Domiciano de Souza, A., "Hot stars mass-loss studied with Spectro-Polarimetric INterferometry (SPIN)," *A&A* **410**, 375–388 (Oct. 2003).

[20] Quirrenbach, A., Bjorkman, K. S., Bjorkman, J. E., Hummel, C. A., Buscher, D. F., Armstrong, J. T., Mozurkewich, D., Elias, N. M., I., and Babler, B. L., "Constraints on the Geometry of Circumstellar Envelopes: Optical Interferometric and Spectropolarimetric Observations of Seven Be Stars," *ApJ* **479**, 477–496 (Apr. 1997).

[21] Monnier, J. D., Le Bouquin, J.-B., Anugu, N., Kraus, S., Setterholm, B. R., Ennis, J., Lanthermann, C., Jocou, L., and ten Brummelaar, T., "MYSTIC: Michigan Young STar Imager at CHARA," in [*Optical and Infrared Interferometry and Imaging VI*], Creech-Eakman, M. J., Tuthill, P. G., and Mérand, A., eds., *Society of Photo-Optical Instrumentation Engineers (SPIE) Conference Series* **10701**, 1070122 (July 2018).

[22] Traub, W. A., "Polarization effects in stellar interferometers.," in [*European Southern Observatory Conference and Workshop Proceedings*], *European Southern Observatory Conference and Workshop Proceedings* **29**, 1029–1038 (Jan. 1988).

[23] Bagnuolo, Jr, W. G., "The CHARA Array, Final Report to the National Science Foundation, Appendix D," tech. rep., CHARA, Georgia State University, Atlanta (1994). http://chara.gsu.edu/astronomers/technical-reports.

[24] Ridgway, S. T. and Bagnuolo, Jr, W. G., "Polarization Revisited," Tech. Rep. 28, CHARA, Georgia State University, Atlanta (1996). http://chara.gsu.edu/astronomers/technical-reports.

[25] Labdon, A., Monnier, J. D., Kraus, S., Le Bouquin, J.-B., Setterholm, B. R., Anugu, N. A., ten Brummelaar, T. A., Lanthermann, C., Davies, C. L., Ennis, J., Gardner, T., Schaefer, G. H., Sturmann, L., and Sturmann, J., "A new frontier for J-band interferometry: Dual-band NIR interferometry with MIRC-X," in [*Optical and Infrared Interferometry and Imaging VII*], Tuthill, P. G., Mérand, A., and Sallum, S., eds., *Society of Photo-Optical Instrumentation Engineers (SPIE) Conference Series* (Dec. 2020).

[26] Anugu, N., Le Bouquin, J.-B., Monnier, J. D., Kraus, S., Setterholm, B. R., Labdon, A., Lanthermann, C., Ennis, J., Davies, C. L., ten Brummelaar, T. A., Schaefer, G. H., Sturmann, J., and Anderson, M. D., "CHARA/MIRC-X - a high-sensitive six telescope interferometric imager concept, commissioning, and early science," in [*Optical and Infrared Interferometry and Imaging VII*], Tuthill, P. G., Mérand, A., and Sallum, S., eds., *Society of Photo-Optical Instrumentation Engineers (SPIE) Conference Series* (Dec. 2020).